

Benniston AC, Tkachenko NV, Lemmetyinen H, He X.

[Charge Shift, Charge Recombination and Triplet Formation in a Closely-Spaced Molecular Dyad based on a Borondipyrromethene \(Bodipy\) and an Expanded Acridinium Cation.](#)

ChemPhotoChem 2017

DOI: <https://doi.org/10.1002/cptc.201700184>

Copyright:

This is the peer reviewed version of the following article: Benniston AC, Tkachenko NV, Lemmetyinen H, He X. Charge Shift, Charge Recombination and Triplet Formation in a Closely-Spaced Molecular Dyad based on a Borondipyrromethene (Bodipy) and an Expanded Acridinium Cation. *ChemPhotoChem* 2017, which has been published in final form at <https://doi.org/10.1002/cptc.201700184>. This article may be used for non-commercial purposes in accordance with Wiley Terms and Conditions for Self-Archiving.

DOI link to article:

<https://doi.org/10.1002/cptc.201700184>

Date deposited:

01/12/2017

Embargo release date:

01 December 2018

Charge Shift, Charge Recombination and Triplet Formation in a Closely-Spaced Molecular Dyad based on a Borondipyrromethene (Bodipy) and an Expanded Acridinium Cation

Xiaoyan He,^[a] Andrew C. Benniston,^{*[a]} Helge Lemmetyinen^[b] and Nikolai V. Tkachenko^{*[b]}

Abstract: A molecular mono-cationic dyad comprising a borondipyrromethene (Bodipy) and an expanded planar acridinium cation was prepared. The dyad when excited in solution by an ultrashort laser pulse generates a charge shift state, where a positive charge is transferred to the Bodipy from the acridinium subunit. The process takes less than 1ps in MeCN and around 8 ps in 1,2-dichloroethane. The charge shift state collapses, in part, back to the ground state but it also leads to partial triplet formation; the discrimination between rates for the forward and reverse processes is ca. 7.

Introduction

Closely-spaced donor-acceptor dyads are envisaged as the simplest molecular systems for supporting light capture and coupled charge separation.^[1] There has been speculation that by meticulous design of molecular dyads, electron transfer processes can be optimised to support efficient temporal charge separation.^[2] Certainly this notion has appeal because of the potential simplicity for synthesising such molecular systems, and their applications in areas such as dye sensitized solar cells (DSSCs).^[3] To have universal appeal, dyads which absorb over a wide range of the visible spectrum, and still support efficient charge separation, are highly sought after.^[4] One chromophore which meets requirements for dyad production is the borondipyrromethene (Bodipy) subunit.^[5] The robust basic dye absorbs strongly in the region around 500 nm, is intensely fluorescent with a high quantum yield and readily functionalised

at different locations on the dye's core.^[6] The Bodipy segment will perform as an electron donor or acceptor in the excited state

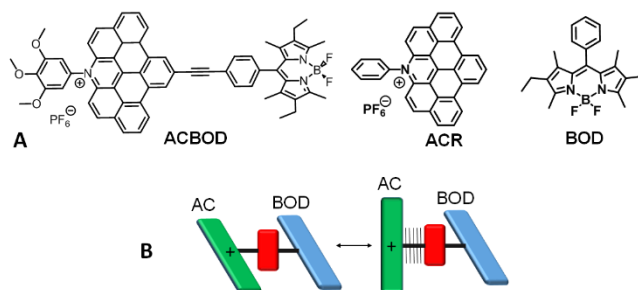


Figure 1. The model Bodipy-expanded acridinium dyad, **ACBOD**, and the control compounds **ACR** and **BOD** (A) and simple cartoon to represent the two extreme mutual orientations of the end units (B). Note: the red unit represents the phenyl group which in the ground and excited state is kept orthogonal to the Bodipy by the two methyl groups and can couple to the expanded acridinium when they are both in-plane.

depending on the nature of the group attached to the dye.^[7] It is critical for any working device based on, for example, a DSSC that the radical ion pair generated after photoexcitation is stable towards degradation because of side reactions (e.g., proton loss).^[8] The fully alkylated Bodipy (**BOD**) moiety meets this requirement because of its highly reversible oxidation/reduction electrochemistry.^[9] In the search for a very robust electron acceptor the expanded acridinium (**ACR**) subunit was established as a superior version of this moiety.^[10] The reversible electrochemistry of **ACR** and its favourable long-wavelength absorption profile, reasonable fluorescence quantum yield are highly beneficial traits.^[11] In addition, the internal reorganisation energy associated with formation of the radical is minimised because of the rigidity of the planar aromatic group. By the combination of the two molecular components the dyad **ACBOD** was designed and produced (Figure 1A). Within the design element there are several key features including the phenyl spacer at the meso position of the Bodipy, which is held orthogonal to the dipyrromethene core by the methyl groups.^[12] Such a feature is expected to decouple the **ACR** and **BOD** units, at least in the ground state, when they are both co-planar (Figure 1B-left). The low-energy activated free rotation of the **ACR** group at the acetylene unit does, however, facilitate conjugation with the phenyl spacer (Figure 1B-right). These two extreme geometries were projected to play a role in the photoinduced electron transfer

[a] Prof A. C. Benniston,* Dr X. He
Molecular Photonics Laboratory, Chemistry-School of Natural & Environmental Sciences
Newcastle University
Newcastle upon Tyne, NE1 7RU, UK
E-mail: andrew.benniston@ncl.ac.uk

[b] Prof N. V. Tkachenko,* Prof H. Lemmetyinen
Laboratory of Chemistry & Bioengineering
Tampere University of Technology
PO Box 541, Tampere, FIN-33101, Finland
E-mail:nikolai.tkachenko@tut.fi

Supporting information for this article is given via a link at the end of the document.

processes, too. Upon excitation of either moiety a charge shift via electron transfer was anticipated to leave a cation radical at the Bodipy site. Whereas fast charge shift is desirable and requires effectual π -conjugation, the reverse reaction (i.e., charge recombination) is more likely curtailed in an orthogonal geometry.^[13] However, a drawback for the latter case is the potential for localised triplet formation on one of the components, which can accompany the charge recombination process.^[14] For **ACBOD** as well as probing both charge shift and recombination our aim was to determine if localised triplet formation was significant, and what affect, if any, solvent played in the process. The final design feature is the trimethoxyphenyl group which when deprotected affords a potential anchoring site to a semiconductor surface for DSSC applications.

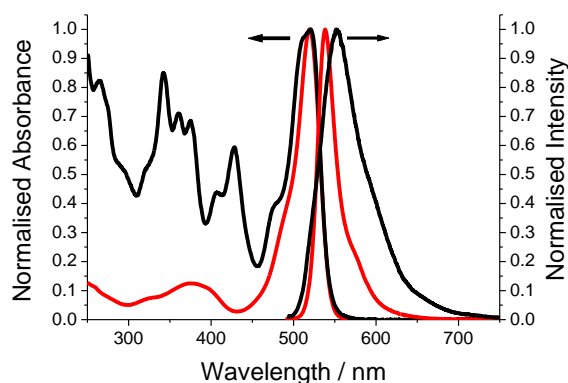


Figure 2. Room temperature absorption and fluorescence spectra for **ACBOD** (black) and **BOD** (red) in MeCN. $\lambda_{\text{ex}} = 480$ nm.

Results and Discussion

The dyad was prepared using starting materials and standard protocols published previously (see Supporting Information).^[15] The ^1H NMR spectrum for **ACBOD** displayed typical resonances at $\delta = 4.03$ and 3.95 ppm for the OMe groups of the aryl group, including aromatic signals for the expanded acridinium subunit. The ^{11}B and ^{19}F NMR spectra were fully consistent with identification of the Bodipy segment. The absorption/fluorescence profiles for **ACBOD** in MeCN are shown in Figure 2, and for comparison the corresponding spectra for meso-phenyl Bodipy are highlighted. The absorption envelope consists of localised π - π^* electronic transitions associated with both the **BOD** and **ACR** subunits. The series of sharp absorption bands below ca. 450 nm are predominantly based on the **ACR** subunit. Because of these electronic transitions the harvesting of photons is covered towards the blue, especially since Bodipy contains no strong absorption in this region. The dominant low-energy narrow absorption band located at 521 nm is primarily associated with the S_0 - S_1 electronic transitions for the Bodipy; the slight broadness is a result of two underlying absorptions from **ACR** (see Supporting Information). Extremely weak fluorescence at $\lambda_{\text{max}} = 553$ nm is observed from **ACBOD** in dilute MeCN ($\phi_{\text{FLU}} < 0.008$). The band is slightly red shifted and considerably broader^[16] than for Bodipy alone, and is not the result of intersected emission from **ACR** (see

Supporting Information). It is worth noting that emission from **ACR** overlaps with the absorption profile for **BOD**, and the same argument is valid for **BOD** emission overlapping with **ACR** absorption (see Supporting Information). Within the framework of Förster theory,^[17] forward and reverse electronic energy transfer is feasible between the two distinct chromophore centres. A corrected fluorescence excitation spectrum collected for **ACBOD** in MeCN (see Supporting Information) is a respectable match to the absorption profile, especially highlighting bands associated with the **ACR** subunit; photons collected at the expanded acridinium group appear to be shuttled to the **BOD** group.

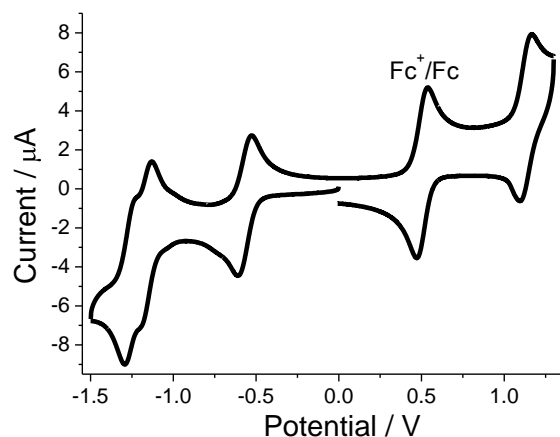


Figure 3. Cyclic voltammogram recorded for **ACBOD** in DCM (0.2 M TBAP) at a glassy carbon working electrode. Scan rate = 50 mVs^{-1} .

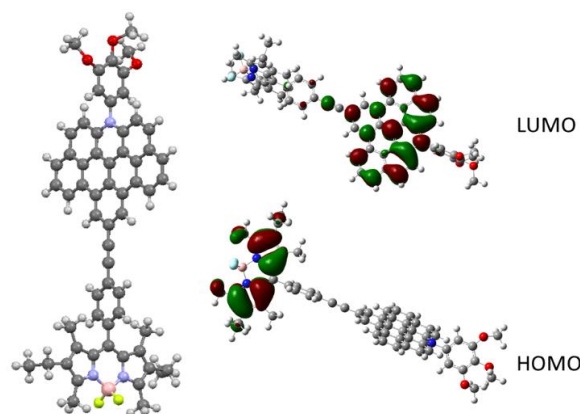


Figure 4. Ball and stick energy-minimised gas-phase structure for **ACBOD** (left) and location of the Kohn-Sham HOMO and LUMO (right) calculated by DFT using B3LYP and a 6-31G basis set.

Confirmation of the favorable reversible electrochemistry of **ACBOD** was obtained using cyclic voltammetry. The cyclic voltammogram collected in dry DCM is illustrated in Figure 3. The reversible wave at $E_1 = +0.62$ (vs Fc^+/Fc) is associated with the one electron BD/BD^+ couple,^[18] whereas the first wave in the reduction side of the cyclic voltammogram at $E_2 = -1.08$ (vs

Fc⁺/Fc) is assigned to one electron redox at the **ACR** site. There are two overlapping waves situated at $E_3 = -1.68\text{V}$ and $E_4 = -1.72\text{V}$ (vs Fc⁺/Fc). The first is tentatively assigned to the BD/BD^{•-} couple and the second to the further one-electron reduction of the neutral **ACR** radical.

The calculated ground-state molecular structure for **ACBOD** using DFT (B3LYP) and a 6-31G basis set is illustrated in Figure 4. The **ACR** and phenyl group are *ca.* 10° away from being coplanar, but very similar energy rotamers are possible by rotation of the **ACR** group at the acetylene carbon. The angle between the planes comprising the meso-phenyl and dipyrromethene subunits is 88.7°, supporting the conception that the **ACR** and **BOD** groups may couple only weakly in the ground state. Also illustrated in Figure 4 are representations of selected Kohn–Sham frontier molecular orbitals. The HOMO is located preferentially at the Bodipy site, and as observed in previous calculations contains a node at the meso carbon site. The LUMO is focussed at the **ACR** subunit. Calculations performed using an integral equation formalism polarizable continuum model (IEFPCM) for several solvents, as expected perturbed the energies of the molecular orbitals (Table 1). For all solvents the HOMO-LUMO gap increased to afford an energy gap mapping approximately to a charge transfer (CT) state. The calculated energy gap would appear to be overestimated (*ca.* 0.4 eV) by comparison to the measured value from electrochemistry ($\Delta E = 1.7\text{ eV}$). The significant calculated dipole moments (DMs) (Table 1) for the ground-state are also consistent with the CT character of the dyad.

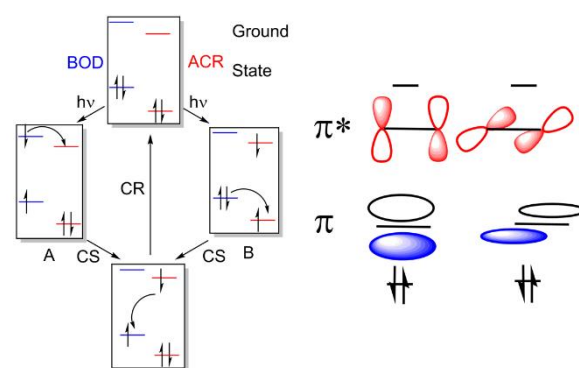
Table 1. Comparison of DFT calculated selected molecular orbitals for **ACBOD** using B3LYP and a 6-31G basis set.

Solvent ^[a]	HOMO / eV	LUMO / eV	Δ / eV ^[b]	DM / D ^[g]
Gas phase	-6.48	-5.54	0.94	31.0
DCE ^[b]	-5.65	-3.45	2.20	35.6
MeCN ^[c]	-5.62	-3.27	2.35	36.1
THF ^[d]	-5.68	-3.54	2.14	35.3
DCM ^[e]	-5.66	-3.48	2.18 (1.7) ^[f]	35.5

[a] Calculated using the IEFPCM. [b] Difference in energy between HOMO and LUMO. [c] 1,2-Dichloroethane. [d] Tetrahydrofuran. [e] Dichloromethane. [f] Calculated value from electrochemistry experiments in bracket. [g] Ground state dipole moment in Debye.

Evidence from both the electrochemistry findings and the DFT calculations are consistent with a CT state lower in energy than the excited singlet states localised on either subunit in **ACBOD**, especially in polar solvents. The overall low fluorescence quantum yield for the Bodipy unit within the compound is also

consistent with efficient deactivation of its first-excited singlet state. Using previous findings^[19] a basic charge-shift process is conceivable depending on which chromophore is excited; namely, electron transfer from the first-singlet excited state of **BOD** to **ACR**, process A, or reduction of the first-singlet excited state of **ACR** by electron transfer from **BOD**, process B. Both cases would produce a similar CT state: positive charge shift to the **BOD** site (Scheme 1). It is noted that process A is facilitated through the LUMO π^* orbitals of the bridge whereas process B (hole transfer) is mediated by the HOMO orbitals. Even by inspection of the basic MO picture for acetylene (Scheme 1) we might expect that process B would be favoured via the filled π orbitals which span across the two carbon atoms. In contrast, the node observed in the π^* orbital picture is likely less favoured to promote process A. The charge recombination process is doubtless via intervention of the π^* orbitals.



Scheme 1. A basic representation of processes that can take place after excitation of **ACBOD** via the two separate chromophore units (left) and a simple representation of select molecular orbitals for an acetylene subunit.

To gain insight into the photoprocesses the technique of femtosecond pump-probe spectroscopy was used. Excitation of a sample of **ACBOD** in DCE with an ultrashort laser pulse afforded transient spectra with selected temporal profiles shown in Figure 5A. As well as a clear bleaching at *ca.* 520 nm positive features toward the blue part of the spectrum grow-in and decay over ultrashort timescales. The bleaching effect is very clear which persists over long time scales. Transient changes measured at 520 nm show an increase in bleaching over some 10 ps followed by a bi-exponential decay (Figure 5A-insert). Differential transient spectra obtained from a least-squares global fit to a three exponential model are illustrated in Figure 5B. The blue circle short-lived component represents formation of the CT state with an associated lifetime for charge shift $\tau_{CS} = 7.8\text{ ps}$ ($k_{CS} = 1.3 \times 10^{11}\text{ s}^{-1}$). The red triangle profile is taken to depict charge recombination with a lifetime $\tau_{CR} = 54\text{ ps}$ ($k_{CR} = 1.9 \times 10^{10}\text{ s}^{-1}$). The long-lived component (green open circles) is assigned to a localised triplet state by comparison to findings from our previous work. Time-resolved spectroscopic data collected in limited solvents of various polarity were analysed in the same manner (see Supporting Information) and parameters from the fits are shown in Table 2. It is noted that formation of the CT state was too fast to accurately measure in MeCN.

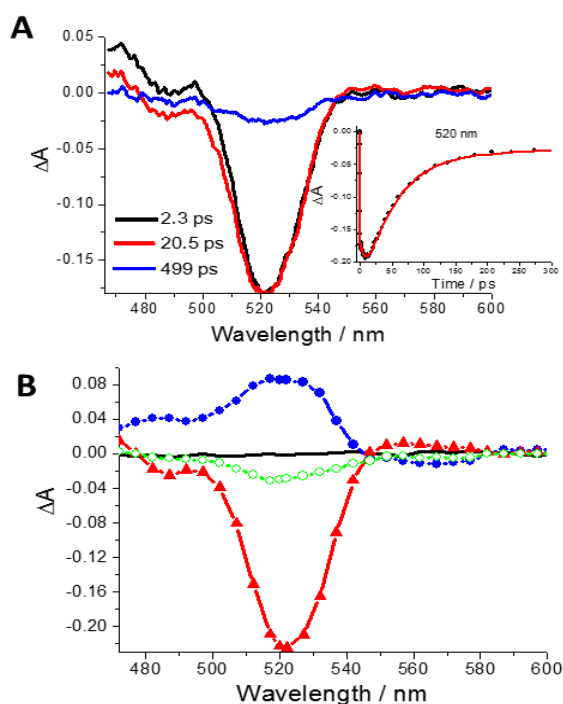


Figure 5. A: Selected transient absorption spectra recorded at three different delay times for **ACBOD** in DCE following laser excitation with a 70fs laser pulse delivered at 415 nm (insert shows decay (●) and fit (-) to a three exponential model). B: Global fit calculated differential transient absorption spectra. Blue circle (7.8 ps), red triangle (54 ps) and green open circle (> 1 ns).

Given the wealth of information on modelling electron transfer in terms of semi-classical Marcus theory,^[20] it is reasonable to conclude that charge separation is occurring in the Marcus normal region ($-\Delta G_{CS} \sim 0.63$ eV). Charge recombination is governed by intersecting potential energy surfaces within the Marcus inverted region ($-\Delta G_{CR} \sim 1.7$ eV). The timescale for charge separation is evidently slower than the solvent longitudinal relaxation time (τ_L) (Table 2), which reflects the relaxation of polarization within a dielectric continuum subjected to a charge perturbation. It is noticeable that τ_{CS} is at a maximum when τ_L is too, but over the limited solvent range there is only a tentative correlation between the two parameters (see Supporting Information).^[21] The Debye relaxation time (τ_D) which represents disparate molecular motions does not match that favourably with τ_{CS} except for the case of DCE. Because of the strong ground-state dipole moment there is likely specific orientation of polar solvent molecules (i.e., MeCN, BuCN, THF) at both the expanded acridinium and Bodipy sites. Following charge shift the large flat expanded acridinyl radical is more prone to experience a fluctuation in the solvent sphere (Figure 6); in contrast the Bodipy site will be likely less affected. The solvent DCE is interesting since in its anti-form (trans) the dipole moment is zero, but in the

gauche-form the dipole moment is 2.63D. The experimental dipole moment is 1.47D and corresponds to the mean-square dipole moment of the equilibrium mixture (31% gauche, 69% anti).^[22] This equilibrium mixture is probably affected by the clustering of DCE molecules around the ground-state structure of **ACBOD**, since anti to gauche conversion by rotation around the C-C bond will provide the necessary dipoles to support the positive charges. Following charge shift the DCE solvent sphere around the expanded acridinyl radical is likely to return to the equilibrium gauche:anti ratio. The similarity of τ_{CS} and τ_D for DCE may be a consequence of such perturbations of the equilibrium mixture.

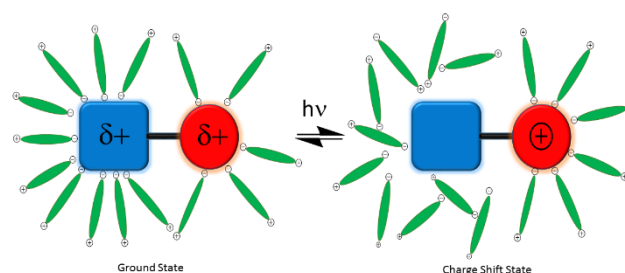


Figure 6. Simplified representation of polar solvent orientation within **ACBOD** before and after light activation.

The discrimination k_{CS}/k_{CR} is very modest (ca. 7) and the ratio remains relatively constant for the solvent series. The ratio is certainly smaller than our previous finding for an analogous dyad comprising a 1,2,3-trimethoxybenzene donor linked to the expanded acridinium via an acetylene bridge ($k_{CS}/k_{CR} = 16$).^[23] The triple bond linker would appear to be too efficient a conduit for the exchange of electrons and is in fitting with previous studies.^[24]

Table 2. Comparison of DFT calculated selected molecular orbitals for **ACBOD** using B3LYP and a 6-31G basis set.

Solvent	$\epsilon^{[a]}$	$\eta^{[b]}$ /cP	$\tau_L^{[c]}$ /ps	$\tau_D^{[d]}$ /ps	τ_{CS} /ps	τ_{CR} /ps	$k_{CS}/k_{CR}^{[e]}$	$\phi_T^{[f]}$ / %
MeCN ^[g]	37.5	0.34	-0.2	3.3	<1	14	-	15
BuCN ^[h]	20.7	0.62	0.53	6.2	2.5	17	6.8	7
DCE ^[i]	10.4	0.83	1.6	6.9	7.8	54	6.9	13
THF ^[k]	7.58	0.46	0.8	3.1	5.4	36	6.7	9

[a] Static dielectric constant. [b] Dynamic viscosity. [c] Solvent longitudinal relaxation time. [d] Debye relaxation time. [e] Ratio for rates of charge separation and charge recombination. [f] Quantum yield of triplet estimated from femtosecond pump-probe experiments. [g] Acetonitrile. [h] Butyronitrile. [i] 1,2-Dichloroethane. [k] Tetrahydrofuran.

In work by us^[25] and others^[26] the formation of a localized triplet state accompanying charge recombination is well documented and is essentially an energy wasting process, although recently the method for triplet formation and singlet oxygen production has become popular.^[27] The crude triplet yields (Table 2) are modest and there is no obvious trend within the limited solvent series. For instance, both low and high viscous solvents appear to be just as effective at triplet formation. The mechanism for triplet formation via charge recombination is heavily linked to geometry and is especially favoured in orthogonally arranged donor-acceptor systems. The spin-flip required is facilitated by spin-orbit coupling and presumably there is a nest of orthogonal conformers which dominate in solvents such as MeCN and DCE following light-initiated charge shift. It is noted that triplet formation is still not the main relaxation pathway and regeneration of the ground state still dominates in the dyad.

Conclusions

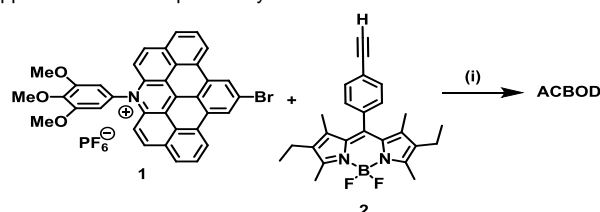
The coupling of the expanded acridinium unit to a fully alkylated Bodipy group affords a way to capture photons with energies up to ca. 2 eV, with the acridinium acting as the primary absorber of photons below 450 nm and an excellent electron acceptor. This is a positive feature of utilising expanded acridinium groups over the basic acridinium or smaller quinolinium subunits. Unfortunately, the charge shift state that is generated rapidly in disparate solvents by light activation collapses quickly and would seem to preclude the usefulness of the dyad in artificial photosynthesis applications. The triple bond responsible for maintaining the structural rigidity of the dyad and acting as the electron conduit is far from ideal. Surface attachment of the dyad to an n- or p-type semiconductor, depending on which way around the system is attached, could be a solution by hopefully promoting rapid electron or hole removal. Alternatively, insertion of partial decoupling group between the **ACR** and **BOD** moieties would help increase separation distance between the two groups and curtail the charge shift and recombination processes. There is also a necessity to reduce significantly the energy wasting triplet forming activity. This latter feature is very much tied into structural features of the dyad and the relative orientation of the two subunits.

Experimental Section

General

Bulk chemicals were purchased at the highest purity possible from Sigma-Aldrich and used as received unless otherwise stated. Tetra-n-butylammonium hexafluorophosphate (TBAP) purchased from Sigma-Aldrich was recrystallized several times from methanol and dried thoroughly under vacuum before being stored in a desiccator. Standard solvents were dried by literature methods before being distilled and stored under nitrogen over 4 Å molecular sieves. Spectroscopic-grade solvents were used in all fluorescence/absorption-spectroscopy measurements. ¹H, ¹⁹F and ¹¹B NMR spectra were recorded with either Bruker AVANCE III

300 MHz, JEOL ECS-400 MHz or Bruker AVANCE III HD 700 MHz spectrometers. Chemical shifts for ¹H spectra are referenced relative to the residual deuterated solvent. Routine mass spectra and elemental analyses were obtained using in-house facilities. Absorption spectra were recorded using a Hitachi U3310 spectrophotometer and corrected fluorescence spectra were recorded using a Lambda Advanced F 4500 spectrometer. Cyclic voltammetry experiments were performed using a fully automated CH Instruments Electrochemical Analyzer and a three electrode set-up consisting of a glassy carbon working electrode, a platinum wire-counter electrode and a sodium saturated calomel reference electrode (SSCE). All studies were performed in deoxygenated DCM containing TBAP (0.1 M) as background electrolyte. The solute concentrations were typically 0.3 mM. Redox potentials were reproducible to within ±15 mV. Pump-probe experiments were carried out using apparatus described previously.^[28]



Scheme 2. Reagents and Conditions: (i) Pd(PPh₃)₄, CuI, DMF, Et₃N, 80°C, 30h, 19% yield.

Synthesis

Compounds **1**^[29] and **2**^[30] were prepared by literature methods and the preparation of **ACBOD** is shown in Scheme 2.

Preparation of ACBOD

Compounds **1** (30 mg, 0.040 mmol) and **2** (16.3 mg, 0.040 mmol) were dissolved in DMF (6 mL) followed by the addition of triethylamine (3 mL). The mixture was bubbled with nitrogen for 15 minutes before being heated to 80 °C. Then Pd(PPh₃)₄ (4 mg, 9%) and copper(I) iodide (0.7 mg, 9%) were added, and the resulting mixture was further heated and stirred overnight (20 hours). Another portion of catalyst (i.e., Pd(PPh₃)₄ (4 mg, 9%) and copper(I) iodide (0.7 mg, 9%)) was added and the reaction was left for another 10 hours. After cooling to room temperature distilled water was added to the mixture to help the precipitation of the product. The solvent was removed and the residue was dissolved in dichloromethane, washed with water, dried over magnesium sulphate and the solvent was removed under vacuum to afford a dark red crude product. The crude product was purified by column chromatography (aluminium oxide, basic activated) eluting with dichloromethane / petroleum ether = 1 / 1, dichloromethane, dichloromethane / acetone = 20 / 1, 10 / 1 and gradually increasing the ratio to 7 / 1. Yield, 8 mg, 0.0075 mmol, 19%. ¹H NMR (400 MHz, CD₃CN): δ = 8.93 - 8.91 (d, *J* = 8.0 Hz, 2H), 8.68 - 8.66 (d, *J* = 9.2 Hz, 2H), 8.63 (s, 2H), 8.51 - 8.49 (d, *J* = 8.0 Hz, 2H), 8.21 - 8.17 (t, *J* = 8.0 Hz, 2H), 8.03 - 8.01 (d, *J* = 9.2 Hz, 2H), 7.81 - 7.79 (d, *J* = 8.0 Hz, 2H), 7.42 - 7.40 (d, *J* = 8.0 Hz, 2H), 7.17 (s, 2H), 4.03 (s, 3H), 3.95 (s, 6H), 2.27 (s, 6H), 2.23 - 2.17 (q, *J* = 7.6 Hz, 4H), 1.34 (s, 6H), 0.95 - 0.91 (t, *J* = 7.6 Hz, 6H) ppm. ¹¹B NMR (CD₃CN, 128 MHz): δ (ppm) = (-0.33) - (-0.83) (t, *J*_{B-F} = 32 Hz) ppm. ¹⁹F NMR (CD₃CN, 367 MHz): δ (ppm) = -71.86 to -73.74 (d, *J*_{P-F} = 690 Hz), -144.99 to -145.25 (q, *J*_{F-B} = 32 Hz) ppm. ³¹P NMR (CD₃CN, 162 MHz): δ (ppm) = -130.94 to -57.13 (sep, *J*_{P-F} = 707 Hz). MALDI: *m/z* calcd for [M-PF₆]⁺: 919.4; found: 919.4.

Acknowledgements

We thank EPSRC sponsored Mass Spectrometry Service at Swansea for the collection of mass spectra and Newcastle University for financial support.

Keywords: Bodipy • Acridinium • Charge Separation • Charge Recombination • Triplet

References

- [1] a) J. C. Bertran, F.-P. Montforts, *Eur. J. Org. Chem.* **2017**, 1608; b) M. Fujitsuka, S. S. Kim, C. Lu, S. Tojo, T. Majima, *J. Phys. Chem. B* **2015**, 119, 7275; c) C. A. Wijesinghe, M. E. El-Khouly, N. K. Subbaiyan, M. Supur, M. E. Zandler, K. Ohkubo, S. Fukuzumi, F. D'Souza, *Chem-Eur. J.* **2011**, 17, 3147; d) H. Imahori, N. V. Tkachenko, V. Vehmanen, K. Tamaki, H. Lemmetyinen, Y. Sakata, S. Fukuzumi, *J. Phys. Chem. A* **2001**, 105, 1750.
- [2] a) M. Yamazaki, Y. Araki, M. Fujitsuka, O. Ito, *J. Phys. Chem. A* **2001**, 105, 8615; b) E. Baranoff, I. M. Dixon, J.-P. Collin, J.-P. Sauvage, B. Ventura, L. Flamigni, *Inorg. Chem.* **2004**, 43, 3057; c) D. I. Schuster, P. Cheng, P. D. Jarowski, D. M. Guldi, C. Luo, L. Echegoyen, S. Pyo, A. R. Holzwarth, S. E. Braslavsky, R. M. Williams, G. Klichm, *J. Am. Chem. Soc.* **2004**, 126, 7257.
- [3] J. R. Durrant, S. A. Haque, E. Palomares, *Chem. Soc. Rev.* **2006**, 3279.
- [4] a) M. Fujitsuka, N. Tsuboya, R. Hamasaki, M. Ito, S. Onodera, O. Ito, Y. Yamamoto, *J. Phys. Chem. A* **2003**, 107, 1452; b) D. M. Guldi, C. Luo, N. A. Kotov, T. Da Ros, S. Bosi, M. Prato, *J. Phys. Chem. B* **2003**, 107, 7293.
- [5] a) R. Ziessel, G. Ulrich, A. Harriman, *New. J. Chem.* **2007**, 31, 496; b) N. Boens, V. Leen, W. Dehaen, *Chem. Soc. Rev.* **2012**, 41, 1130; c) H. Lu, J. Mack, Y. Yang, Z. Shen, *Chem. Soc. Rev.* **2014**, 43, 4778; d) A. Treibs F. H. Kreuzer, *Justus Liebigs Ann. Chem.* **1969**, 721, 116.
- [6] a) D. T. Gryko, D. Gryko, C.-H. Lee, *Chem. Soc. Rev.* **2012**, 41, 3780; b) A. Bassette, G. S. Hanan, *Chem. Soc. Rev.* **2014**, 43, 3342; c) N. Boens, B. Verbelen, W. Dehaen, *Eur. J. Org. Chem.* **2015**, 6577.
- [7] a) S. Hattori, K. Ohkubo, Y. Urano, H. Sunahara, T. Nagano, Y. Wada, N. V. Tkachenko, H. Lemmetyinen, S. Fukuzumi, *J. Phys. Chem. B* **2005**, 109, 15368; b) D. Frath, J. E. Yarnell, G. Ulrich, F. N. Castellano, R. Ziessel, *ChemPhysChem* **2013**, 14, 3348; c) J.-F. Lefebvre, X.-Z. Sun, J. A. Calladine, M. W. George, E. A. Gibson, *Chem. Commun.* **2014**, 50, 5258.
- [8] K. Sahested, J. Holcman, *J. Phys. Chem.* **1978**, 82, 651.
- [9] A. B. Nepomnyashchii, A. J. Bard, *Acc. Chem. Res.* **2012**, 45, 1844.
- [10] a) H. van Willigen, G. Jones II, M. S. Farahat, *J. Phys. Chem.* **1996**, 100, 3312; b) G. Jones II, D.-X. Yan, D. J. Gosztola, S. R. Greenfield, M. R. Wasielewski, *J. Am. Chem. Soc.* **1999**, 121, 11016.
- [11] D. Wu, W. Pisula, M. C. Haberecht, X. Feng, K. Müllen, *Org. Lett.* **2009**, 11, 5686.
- [12] G. J. Hedley, A. Ruseckas, A. C. Benniston, A. Harriman, I. D. W. Samuel, *J. Phys. Chem. A* **2015**, 119, 12665.
- [13] M. S. Rodríguez-Morgade, M. E. Plonska-Brzezinska, A. J. Athans, E. Carbonell, G. de Miguel, D. M. Guldi, L. Echegoyen, T. Torres, *J. Am. Chem. Soc.* **2009**, 131, 10484.
- [14] A. Harriman, L. J. Mallon, G. Ulrich, R. Ziessel, *ChemPhysChem* **2007**, 8, 1207.
- [15] a) A. C. Benniston, D. Rewinska, *Org. Biomol. Chem.* **2006**, 4, 3886; b) D. Wu, X. Feng, M. Takase, M. C. Haberecht, K. Müllen, *Tetrahedron* **2008**, 64, 11379.
- [16] The broad profile was fitted to a standard emission model to afford the following parameters: $E_{00} = 2.4$ eV, solvent reorganisation energy (λ_s) = 0.112 eV, vibrational fundamental ($h\omega$) = 1315 cm^{-1} and Huang-Rhys factor (S) = 0.437. Given that the fully charge transfer state is likely to be lower in energy than 2.4 eV we discount that the emission is from charge recombination. The broadness is probably associated with a structural change that facilitates electron delocalisation onto the Bodipy chromophore.
- [17] a) K. Sienicki, M. A. Winnik, *Chem. Phys.* **1988**, 121, 163; b) P. Woolley, K. G. Steinhäuser, B. Epe, *Biophys. Chem.* **1987**, 26, 367; c) K. Sienicki, *J. Phys. Chem.* **1990**, 94, 1944.; d) D. Bai, A. C. Benniston, V. L. Whittle, H. Lemmetyinen, N. V. Tkachenko, *ChemPhysChem* **2014**, 15, 3089.
- [18] A. B. Nepomnyashchii, S. Cho, P. J. Rossky, A. J. Bard, *J. Am. Chem. Soc.* **2010**, 132, 17550.
- [19] a) G. Jones II, M. S. Farahat, S. R. Greenfield, D. J. Gosztola, M. R. Wasielewski, *Chem. Phys. Lett.* **1994**, 229, 40; b) G. Jones II, D. Yan, J. Hu, J. Wan, B. Xia, V. I. Vullez, *J. Phys. Chem. B* **2007**, 111, 6921.
- [20] R. A. Marcus, N. Sutin, *Biochim. Biophys. Acta, Rev. Bioenerg.* **1985**, 811, 265.
- [21] Within a solvent dependent rate constant model $k_r = A\tau_L^{-\alpha} \exp[-(\Delta G_{is}^* + \Delta G_{os}^*)/RT]$ where A and α are constants and ΔG_{is}^* and ΔG_{os}^* are the Gibbs free energy of activation for the inner sphere (vibrational) and outer sphere (solvent) reorganisation, respectively. Hence, and plot of $\ln k_r$ vs $\ln \tau_L$ will afford a slope = $-\alpha$. A tentative plot for the data in Table 1 affords a value of $\alpha = 1$ which would suggest that charge shift is strongly adiabatic and the contribution of ΔG_{is}^* is small; this latter point is reasonable considering the structure of the dyad.
- [22] M. W. Wong, M. J. Frisch, K. B. Wiberg, *J. Am. Chem. Soc.* **1991**, 113, 4776.
- [23] A. C. Benniston, J. Hagon, X. He, H. Lemmetyinen, N. V. Tkachenko, W. Clegg, R. W. Harrington, *Phys. Chem. Chem. Phys.* **2012**, 14, 3194.
- [24] S. Fraysse, C. Coudret, J.-P. Launay, *J. Am. Chem. Soc.* **2003**, 125, 5880.
- [25] A. C. Benniston, S. Clift, J. Hagon, H. Lemmetyinen, N. V. Tkachenko, W. Clegg, R. W. Harrington, *ChemPhysChem* **2012**, 13, 3672.
- [26] a) M. T. Colvin, A. Butler Ricks, A. M. Scott, D. T. Co, M. R. Wasielewski, *J. Am. Chem. Soc.* **2012**, 116, 1923; b) K. M. Leffler, K. E. Brown, W. A. Salamant, S. M. Dyar, K. E. Knowles, M. R. Wasielewski, *J. Phys. Chem. A* **2013**, 117, 10333; c) V. Bandi, H. B. Gobeze, V. Lakshmi, M. Ravikanth, F. D'Souza, *J. Phys. Chem. C* **2015**, 119, 8095.
- [27] M. A. Filatov, S. Karuthedath, P. M. Polestshuk, H. Savoie, K. J. Flanagan, C. Sy, E. Sitte, M. Telitchko, F. Laquai, R. W. Boyle, M.O. Senge, *J. Am. Chem. Soc.* **2017**, 139, 6282.
- [28] D. Sirbu, C. Turta, A. C. Benniston, F. Abou-Chahine, H. Lemmetyinen, N. V. Tkachenko, C. Wood, E. Gibson, *RSC Adv.* **2014**, 4, 22733.

- [29] A. C. Benniston, X. He, H. Lemmetyinen, N. V. Tkachenko, *RSC Adv.* **2013**, *3*, 4995.
- [30] G. Ulrich, R. Ziesel, *J. Org. Chem.* **2004**, *69*, 2070.
-

